CHAPTER II

THEORETICAL BACKGROUND AND LITERATURE REVIEW

2.1 Motivation for Carbon Dioxide Capture

Global climate change caused by green house gas emission from human activities, is one of the most concerning problems. The primary greenhouse gases include carbon dioxide (CO_2), methane (CH_4), nitrous oxide (N_2O), water vapor (H_2O), ozone (O_3) and chorofluorocarbons (CFC's). Carbon dioxide is clearly a major greenhouse gas that contributes to global warming. In addition to rising levels of atmospheric carbon dioxide, the earth's temperature is increasing. Since carbon dioxide acts as a trap for heat (similar to the glass in a greenhouse), reduction of carbon dioxide emission is an important objective. Global warming potential (GWP) is an indicator used as a relative measure of how much heat a greenhouse gas traps in the atmosphere. It compares the amount of heat trapped by a certain mass of the gas in question to the amount of heat trapped by a similar mass of carbon dioxide. GWP is calculated over a specific time interval, commonly 20, 100 or 500 years. GWP is expressed as a factor of carbon dioxide (whose GWP is set as standard to 1). Table 2.1 shows the global warming potential (GWP) of CH_4, N_2O and HFC-23, relative to CO_2.

Table 2.1 The global warming potential of greenhouse gases (CH_4, N_2O, HFC-23) relative to carbon dioxide

	GWP value		
	time horizon of 20 years	time horizon of 100 years	time horizon of 500 years
Methane	72	25	7.6
Nitrous oxide	289	298	153
HFC-23	12,000	14,800	12,200

For example, the 20-year GWP of CH_4 is 72, meaning that if the same mass of CH_4 and CO_2 were introduced into the atmosphere, the CH_4 will trap 72 times more heat than the CO_2 over the next 20 years.

From Table 2.1, CH_4 and other gases are strong greenhouse gases trapping more heat than CO_2. But the reason why carbon dioxide is still the major greenhouse gas is that there are less amount of CH_4 and other gases in the atmosphere than CO_2 (over 70 % of greenhouse gas emission is from carbon dioxide), as shown in Figure 2.1.

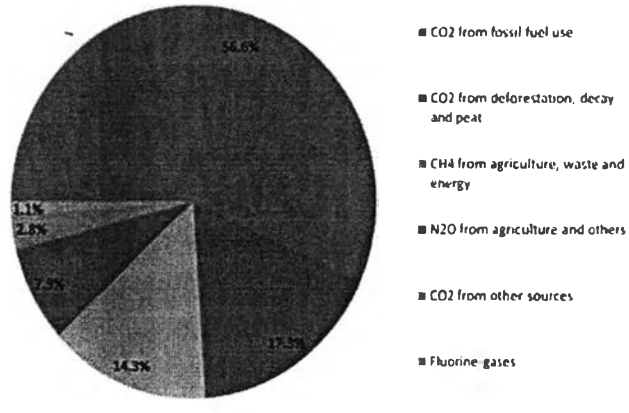

Figure 2.1 Shares of global anthropogenic GHG emission (IPCC, 2007).

Carbon dioxide emission can be quantified in sectors based on human activity, such as industries (chemical and petrochemical manufacturing, cement production, etc), transportation and fossil fuel electric power generation, as shown in Figure 2.2. A large amount of CO_2 is produced from the electricity and heat sectors, responsible for 41 % of world carbon dioxide emission in 2010. Worldwide, this sector relies heavily on coal, the most intensive of fossil fuel, as shown in Figure 2.3. Countries such as Australia, China, India, Poland and South Africa produce between 68 % and 94 % of their electricity and heat through the combustion of coal (IEA, 2012).

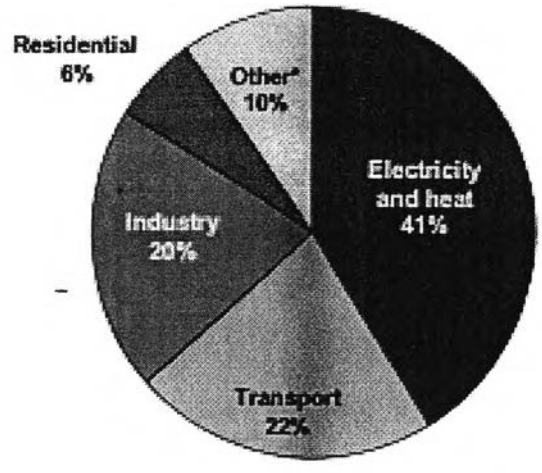

Figure 2.2 World carbon dioxide emissions by sector in 2010 (IEA, 2012).

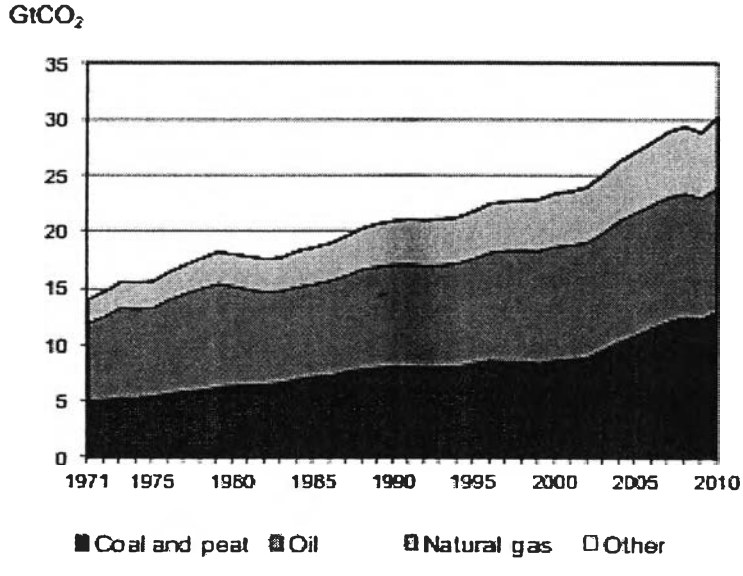

Figure 2.3 Carbon dioxide emissions by fuel in 2010 (IEA, 2012).

Carbon dioxide emission from electricity and heat generation sector accounts for over one third of the total world emission. Therefore, CO_2 capture technologies are significantly needed in this sector to lower CO_2 emission concentrations. The details of CO_2 capture systems are presented in the next section.

2.2 Carbon Dioxide Capture Processes

The main competing technologies for CO_2 capture from fossil fuel usages are:

1) Post Combustion Capture (PCC) from the flue gas of combustion-based plants;
2) Pre Combustion Capture from Syngas in Gasifiction based plants; and
3) Oxy Combustion – the direct combustion of fuel with O_2.

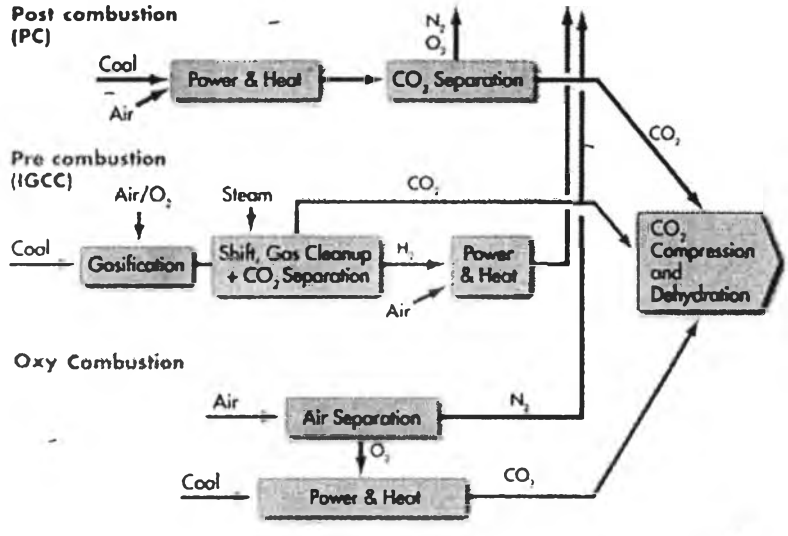

Figure 2.4 Technical options for carbon dioxide capture from coal power plant(Global CCS Institute).

2.2.1 Post-Combustion Carbon Dioxide Capture Process

Post-combustion capture is a downstream process. It involves the removal of CO_2 from the flue gas produced after combustion of the fuel. A diagram of post-combustion capture is shown in Figure 2.4. The oxidant used for combustion is typically air and hence the flue gases are diluted with N_2. The principle of post-combustion capture is to remove CO_2 at a low temperature, low pressure (near atmospheric pressure) and low CO_2 concentration. Since flue gases are at atmospheric pressure, a large volume of gas has to be treated, resulting in large

equipment size and a high capital cost for this process. Typical CO_2 percentage in the flue gas usually depends on combustion systems, as shown in Table 2.2.

Table 2.2 Carbon dioxide partial pressure in flue gas of different combustion system

Flue gas source	CO_2 concentration, vol % (dry)	CO_2 partial pressure, MPa
Natural gas fired boilers	7-10	0.007-0.01
Gas turbines	3-4	0.003-0.004
Oil fired boilers	11-13	0.011-0.013
Coal fired boilers	12-14	0.012-0.014
IGCC after combustion	12-14	0.012-0.014
IGCC synthetic gas after gasification	8-20	0.16-0.14 (before shift)

There are a number of methods for post-combustion CO_2 capture for flue gas. These include:

- Absorption
- Adsorption
- Cryogenic separation
- Membrane separation

2.2.1.1 Absorption

The process of carbon dioxide absorption by a liquid solvent or solid matrix is currently being investigated for scrubbing carbon dioxide from flue gas streams. Absorption is a process that relies on a solvent's chemical affinity with solutes to preferably dissolve one species over another. In carbon dioxide absorption process, a solvent is used to dissolve carbon dioxide, not oxygen, nitrogen gas, or any other components of a flue gas stream. The CO_2-rich solution is pumped to a regeneration column, where the carbon dioxide is stripped from the solution and the solvent recycled. The absorption equipment should be placed after the flue gas desulfurization (FGD) step and before the stack. Optimal conditions for absorption

are low temperature and high pressure, making this the best location of absorption to occur. In addition, most solvents are easily degraded by compounds such as fly ash, other particulates, SOx (SO_2, SO_3, and SO_4) and NO_x (NO_2 and NO_3), so the absorption step must take place after electrostatic precipitation (ESP) and flue gas desulfurization unit (FGD). In a typical absorption process, the CO_2-lean flue gas is either emitted to the atmosphere or possibly used in other applications (e.g., chemical production)

2.2.1.2 Adsorption

Adsorption is another method that can be used to separate carbon dioxide from flue gases generated by fossil fuel power plants. While absorption involves dissolution of carbon dioxide in the solvent, adsorption is a heterogeneous process. Due to interactivity between sorbent and guest molecules, carbon dioxide molecules are attracted and trapped by surface groups of the sorbent or physic-sorbed. Conditions can be manipulated to facilitate adsorption or desorption. Flue gases typically contain N_2, CO_2, H_2O, NO_x, SO_x, CO, O_2 and particulate matter when entering the stack, with concentration varies, depending on the location of the sampling point. Many solids have the capability to selectively adsorb carbon dioxide through small cracks, pores, or just their external surfaces under specific temperature and pressure conditions. Adsorption can be performed on natural substance such as coal or more complex human-made sorbents such as activated carbon, molecular sieves, and zeolite. Figure 2.5 shows an example of an adsorption process.

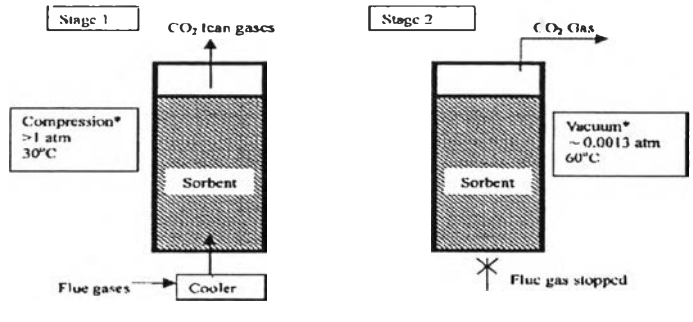

Figure 2.5 Single chamber adsorption system (Douglas, 2005).

The two main methods for adsorption are pressure swing adsorption (PSA) and temperature swing adsorption (TSA). In either case, adsorption rate depends on temperature, partial pressure of carbon dioxide, surface forces (interaction between sorbent and carbon dioxide), and pore size or available surface area of adsorbent. It has been established that PSA is superior to TSA due to its lower energy demand but higher regeneration rate.

2.2.1.3 Cryogenic Separation

Cryogenic is another option for separating carbon dioxide from flue gas in post-combustion carbon dioxide capture system. Flue gas entering the cryogenic system relies on the assumption that all components of the flue gas are removed except for the nitrogen and carbon dioxide prior to cooling. When the other gases and particulates are completely removed, the flue gas that contain mainly carbon dioxide and nitrogen entering to the cryogenic chamber where the temperature and pressure are manipulated in right condition, which is 5.2 bar and -56.6 °C, the triple point for carbon dioxide leading carbon dioxide to condense, while nitrogen remains as a gas and allowing nitrogen to leave the cryogenic chamber. The advantage of this technique is it provides highly concentrated liquid carbon dioxide which can be collected at the bottom of the chamber, but high energy for cooling system is required. Figure 2.6 shows schematic of cryogenic separation process.

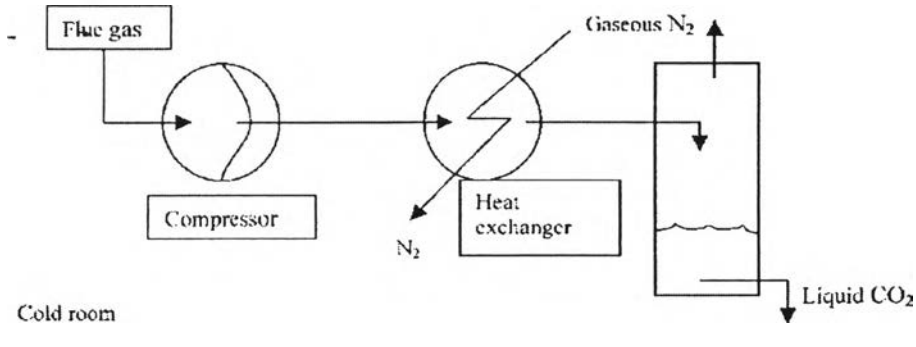

Figure 2.6 Cryogenic separation (Douglas, 2005).

2.2.1.4 Membrane Separation

Membrane separation works on the principle of selective gas permeation with membranes, generally used are polymeric membrane. The flue gas mixture is introduced to the membrane that has two sides. The selective gaseous component will dissolve into the membrane material and diffuses from one side to the other side, while the remaining gas cannot permeate through the membrane. Figure 2.7 shows a schematic of the membrane gas separation.

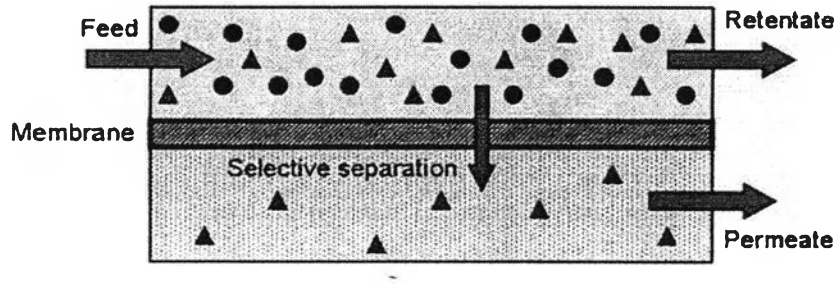

Figure 2.7 Schematic of membrane gas separation (Colin *et al*, 2007).

Table 2.3 Advantages and drawbacks of the technologies for carbon dioxide separation

CO_2 separation technology	Advantages	Drawbacks
Absorption	- Recycling of the sorbent -Non dependence on human operators	-Corrosion of carbon steel facilities due to oxygen -Degradation of the solvent due to SO_x and NO_x
Adsorption	- Recycling of the sorbent - High operation flexibility	- Not able to handle large concentrations of CO_2 - Adsorption also of gases smaller than CO_2
Cryogenic	- No requirement of chemical absorbents	- Several costly steps required to remove all water traces - Increasing layer of solid CO_2 onto heat exchanger surface
Membrane	- No moving parts and modularity -Instantaneous response to variations	- Current low selectivity of membrane material - Limitation on the suitable operating temperature

Table 2.4 Comparison among the four units as function of feed and product conditions (Piewkhaow, 2011)

	Absorption	Adsorption	Cryogenic	Membrane systems
CO_2 in the feed, (mole %)	>5	>10	>5	>15
CO_2 purity, %	>95	75-90	99.99	80-95
CO_2 recovery, %	80-95	80-95	99.99	60-80
Energy requirement, $MJ/kgCO_2$	4-6	5-8	6-10	0.5-6

2.2.2 Pre-Combustion Carbon Dioxide Capture Process

The technology for pre-combustion is widely applied in fertilizer, chemical, gaseous fuel (H_2, CH_4), and power production. In these cases, the fossil fuel is partially oxidized, for instance a gasifier. The resulting syngas (CO, H_2) is shifted into carbon dioxide and hydrogen. The resulting carbon dioxide can be captured from a relatively pure exhaust stream. The hydrogen can now be used as fuel; the carbon dioxide is removed before combustion takes place. In pre-combustion process, carbon dioxide concentration and carbon dioxide partial pressure are both higher than in post-combustion process, so the equipment for the capture process can be smaller than the equipment for the post-combustion capture process.

2.2.3 Oxy-Combustion Carbon Dioxide Capture Process

In oxy-fuel combustion, the fuel is burned in oxygen instead of air. To limit the resulting flame temperature to common levels during conventional combustion, cooled flue gas is re-circulated and injected into the combustion chamber. The flue gas consists mainly carbon dioxide and water vapor, the latter of which is condensed through cooling. The result is an almost pure carbon dioxide stream that can be transport to the sequestration site and stored. Power plant process

based on oxyfuel combustion are sometimes referred to as "zero emission" cycles, because the carbon dioxide stored is not the fraction removed from the flue gas stream (as in the cases of pre- and post-combustion capture) but the flue gas stream itself. The main concerns of the oxyfuel-combustion process are the cost and energy penalty related to its high oxygen requirement.

2.3 Solvents for Chemical Absorption Process

Amine-based carbon dioxide capture from natural gas is well known in the oil and gas industry. Similar plants can be used in the electricity production where carbon dioxide is captured from the flue gas and could be used in several applications. In post-combustion carbon dioxide capture system, amine is one of the most promising solvent to capture carbon dioxide from the flue gas. Carbon dioxide is removed by chemical absorption process by exposing the flue gas to the aqueous amine solution. Carbon dioxide in the flue gas is chemically absorbed with aqueous amine and transformed to a soluble carbonate salt. This reaction is a reversible process. When carbonate salt in the solution is heated in the regeneration step, the reverse reaction occurs. Carbonate salt is transformed back to amine and releases carbon dioxide.

Amines are chemicals that can be described as derivative of ammonia in which one or more of hydrogen atom on the ammonia has been replaced by alkyl group. Amines are classified as primary, secondary and tertiary amines. They are named according to the number of carbon attached to nitrogen. Primary, secondary, and tertiary amines have nitrogen bound to one, two and three carbons, respectively, as shown in Figure 2.8.

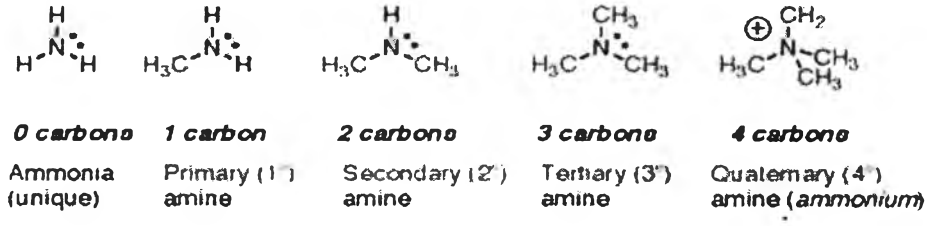

Figure 2.8 Amines: named according to the number of carbons bound to nitrogen.

The most commonly used amines in carbon dioxide capture are Monoethanolamine (MEA), Diethanolamine (DEA), Methyldiethanolamine (MDEA), Diisopropanolamine (DIPA) and Diglycolamine (DGA), their molecular structures are shown in Figure 2.9.

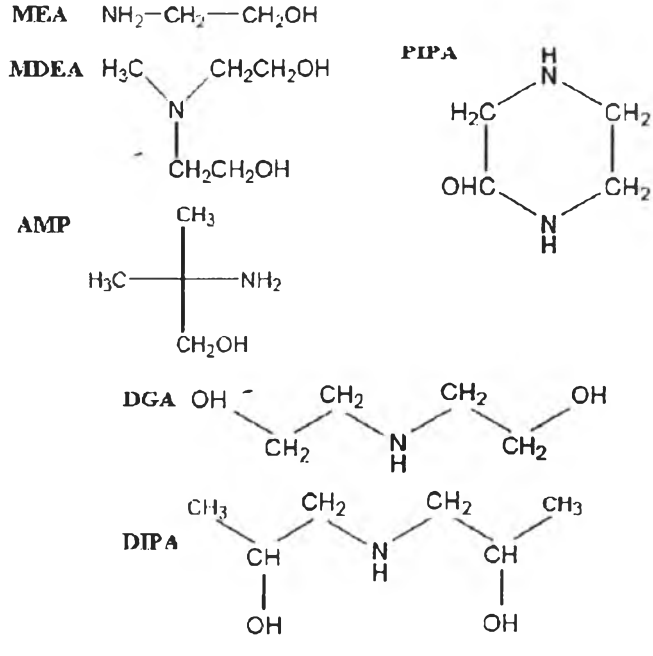

Figure 2.9 Chemical structures of amine commonly used in carbon dioxide capture.

The selection of using aqueous amine depends on many factors, such as physical properties, their performances and cost. Each type of amines has their own advantages and drawbacks.

Primary alkanolamine has the advantage over the other alkanolamines, due to the highest reaction rate with carbon dioxide. One of the most traditional and feasible primary alkanolamine used for carbon dioxide capture and acid gas removal process is monoethanolamine (MEA). Moreover, advantages of MEA are the lowest molecular weight and MEA is the least expensive. Low molecular weight means low viscosity of solvent that is preferable for almost all conventional process. Some drawbacks of monoethanolamine are the highest vapor pressure, strong complex formation between monoethanolamine and carbon dioxide, and high corrosion. High vapor pressure causes a significant loss of solvent; thus a water scrubbing has to be applied to remove some trace of monoethanolamine from CO_2-lean gas back to the system to reduce the solvent loss. Strong complex formation can be described in terms of heat of reaction. Higher strong complex formation means higher heat of reaction that causes more energy required to break up the formation between MEA and CO_2. Due to the high corrosion, the solvent concentration of MEA is limited to 30 wt%.

Table 2.5 Property comparison between primary, secondary and tertiary alkanolamine (Piewkhaow, 2011)

Amines	Reaction rate constant (mol/L.s)	Heat of reaction (kJ/mol CO_2)	stoichio-metric	CO_2 loading
Monoethanolamine (MEA), Primary amine	7,000	90	0.5	0.4
Diethanolamine (DEA), secondary amine	1,000	80	0.5	0.4
Methyldiethanolamine (MDEA), tertiary amine	7	60	1.0	0.5

Secondary alkanolamine has lower reaction rate than primary alkanolamine, but its advantages are less corrosion and lower heat of reaction, so lesser energy is required for the regeneration step than primary alkanolamine.

Tertiary alkanolamine has the lowest reaction rate compared to both primary and secondary alkanolamines. Lower reaction rate causes high circulation rate. An increasing circulation rate is to retain the absorption performance of tertiary alkanolamine. The advantages of this amine are less corrosion and tendency of solvent degradation compared to primary and secondary alkanolamines. Moreover, low heat of reaction of tertiary alkanolamine causes low energy required in the regeneration.

2.4 Monoethanolamine (MEA) Carbon Dioxide Capture Process

Aqueous amine scrubbing is currently considered the most effective, economical and traditional technology that can be used to capture carbon dioxide from post-combustion. Monoethanolamine is one of the most feasible solvent for this purpose. Monoethanolamine carbon dioxide capture process using simple absorption and stripping configuration is shown in Figure 2.10.

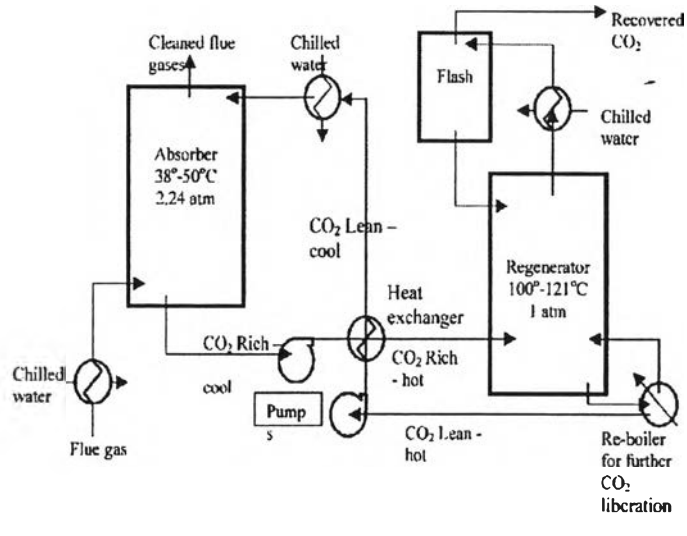

Figure 2.10 Typical chemical absorption process (Douglas, 2005).

The flue gas from the post combustion is cooled prior to entering the absorption column to the temperature between 38 to 50 °C. The pressure can be atmospheric or higher. The temperature of the inlet flue gas is of significant concern. The minimum temperature should be above the condensation point of the gas and the solvent's freezing point. The flue gas entering the column (12-14 vol. %. CO_2, for coal fired boilers) moves upwards countercurrently with lean-amine solvent that enters the top of the column, separating carbon dioxide from the other gases and meeting the specification of the outlet flue gas (such as less than 1.0 vol. % at the exit of the absorber). The flue gas that exits from the absorber is passed through a water scrubber to remove some trace of MEA. Rich-amine solution exits the bottom of the absorber and is pumped through the rich-lean heat exchanger (process heat exchanger) to recover some heat from the hot stream coming from the regenerator and enters the top of the stripping column. In the stripping column, rich-amine is regenerated by hot steam from the reboiler, hence carbon dioxide desorbs from the rich-amine and goes upwards to the top of the stripping column, passing through the condenser to remove trace of water back to the stripping column. The lean-amine after being regenerated exits the bottom of the stripper and is pumped through the rich-lean heat exchanger to transfer heat to rich-amine solvent, and cooled before entering the absorption column for reuse (reusing solvent allows cost reduction; it has no bearing on performance of the solvent unless the solvent degrades with heating). Carbon dioxide with high purity exiting from the stripper is then compressed, cooled and liquefied by a multi-stage compressor before storage and shipment.

Due to the economical and environmental concerns, solvent used for the chemical process must be economical and environmentally friendly. Currently, CO_2 capture is dominated by amine-based technologies, especially MEA, which are high energy intensive and far from environmental point of view due to the emission of the used volatile solvent components. Ionic liquids have been suggested as the promising alternative to conventional volatile solvents due to their low volatility and the other interesting properties. There are many research studies in this area that show the possibility of ionic liquid for CO_2 capture.

2.5 Ionic Liquids

Ionic liquids are a new class of pure ionic, salt-like materials that are liquid at low temperature. Currently, the "official" definition of ionic liquids uses the boiling point of water as a point of reference: "ionic liquids are ionic compound which are liquid below 100 °C". More commonly, ionic liquids have melting points below room temperature; some of them even have melting points below 0 °C are usually called "Room Temperature Ionic Liquid (RTIL)." These new materials are liquid over a wide temperature range (300-400 °C) from the melting point to the decomposition of the ionic liquid.

Compared to a typical ionic liquid, like 1-ethyl-3-methylimidazolium ethylsulfate (m.p. < -20 °C), a typical inorganic salt, e.g., table salt (NaCl, m.p. ≥ 801 °C), is much different in boiling point. The ionic liquid has a significantly lower symmetry, as shown in Figure 2.11. The combination between a bulky unsymmetric cation and an organic or inorganic anion, causes a lower lattic energy compared to ones from typical inorganic salt, resulting in low melting point and becoming a liquid at room temperature. Furthermore, the charge of the cation as well as the charge of the anion is distributed over a large volume of the molecule by resonance. As a consequence, the solidification of the ionic liquid will take place at lower temperatures. In some cases, especially for long aliphatic side chains, a glass transition is observed instead of a melting point.

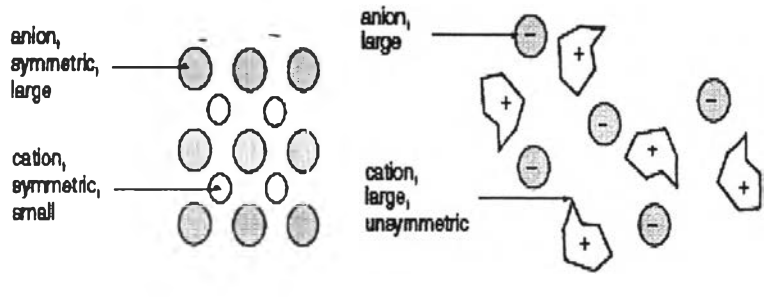

Figure 2.11 Comparison between the configuration of typical inorganic salt (left) and typical ionic liquid (right) (Sigma-Aldrich, US).

The strong ionic interaction within these substances results in a negligible vapor pressure (green solvent), a non-flammable substance, and in a high thermally, mechanically as well as electrochemically stable product. Due to the nonvolatile solvent of ionic liquid, the solvent vapor loss from the system is negligible, making them retain quantitatively in the system and act as a green solvent.

The properties of ionic liquids depend on the combination between the cation and the anion. The type of the cation has a strong impact on the properties of the ionic liquid and will often define the stability, while the type of anion is responsible of the impact on chemistry and functionality (such as gas solubility). This is a unique characteristic of ionic liquids, which can be described as designer solvent due to their structure tunability. The combination of a broad variety of cations and anions leads to a theoretically possible number of 10^8 ionic liquids. However, a more realistic number will be lower magnitude, and approximately 300 are commercially available. Typical structures combining organic cations with inorganic or organic anions are shown in Figure 2.12.

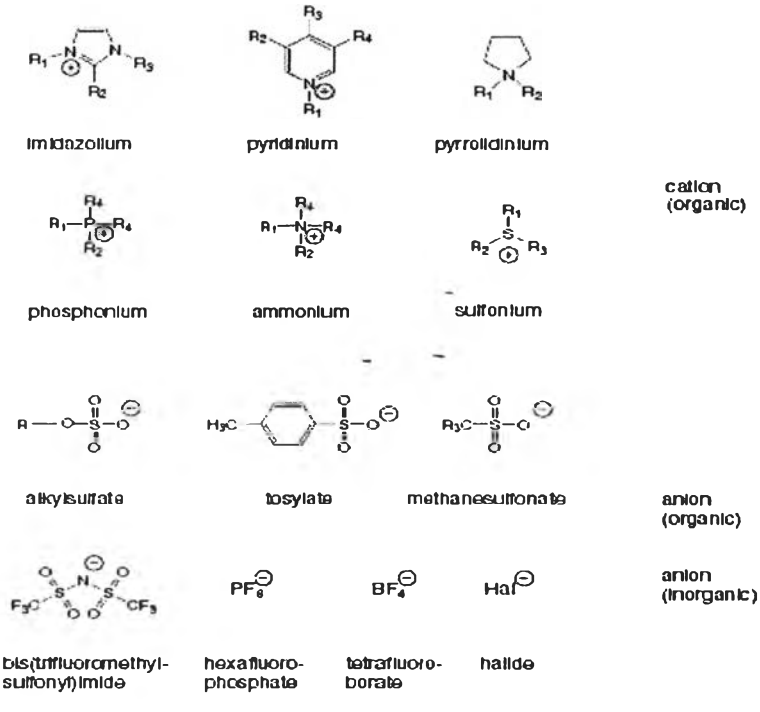

Figure 2.12 Typical structures combine organic cations with inorganic or organic anions (Sigma-Aldrich, US).

Ultimately, the possible combinations of organic cations and anions place chemists in the position to design and fine-tune physical and chemical properties by introducing or combining structural motifs and, thereby, making tailor-made materials possible. Figure 2.13 shows the summary of important properties of ionic liquids and their potential and current applications.

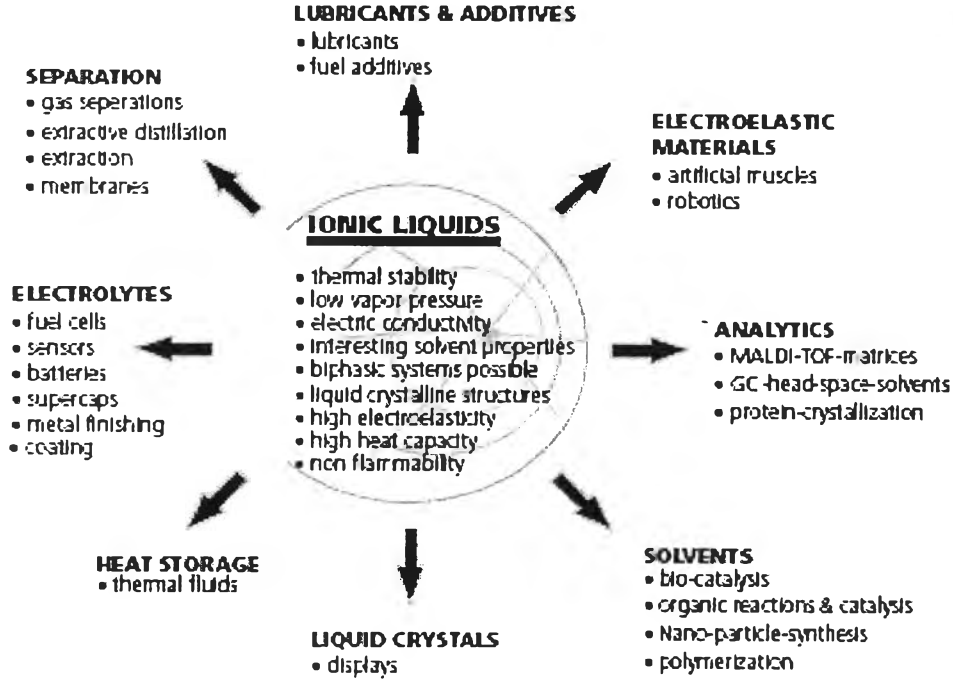

Figure 2.13 Use and application of ionic liquids (Wang *et al.*, 2004).

2.6 Thermodynamic Modeling

In recent years, several different theoretical approaches, correlations and equation of state (EoS) have been used to provide accurate models for appropriate description of thermodynamic properties of ionic liquids. Classical cubic equations, activity coefficient and group contribution methods, quantum chemistry calculations and statistical mechanics based molecular approaches are the models which have been applied to describe the thermodynamic behavior and characteristic of ionic liquid and the solubility of gases in them (Vega *et al.*, 2010). It has been reported that several studies estimated the critical properties of ionic liquids by group contribution methods and used simple cubic equations of state to explain the phase behavior of CO_2 in ionic liquids (Shin and Lee, 2008; Song *et al.*, 2009; Yim *et al.*, 2011). In this section, a group contribution method for critical property estimation, equations of state and an activity coefficient model used in this work will be explained.

2.6.1 Modified Lydersen-Joback-Reid Group Contribution Method

The knowledge regarding the critical properties and other physical parameters of IL is necessary to develop thermodynamic models for pure component and mixtures. For ionic liquids and mixtures comprising ionic liquids, the critical properties cannot be experimentally measured since most of the ionic liquids start to decompose when the temperature approaches the normal boiling point, but such properties are still required to correlate experimental data with thermodynamic model to carry out the simulation of ionic liquid-based CO_2 capture process. The most common method to estimate the critical properties for many substances is the so-called group contribution method, which is used when the critical properties are not available. Several group contribution methods were proposed in the literature. Apparently, a "modified Lydersen-Joback-Reid" method, proposed by Valderrama and Robles (2007), combined the best results for molecules having high molecular weight. This approach considers the equations of Lyndersen for the critical pressure and critical volume, and the equations of Joback-Reid for the normal boiling temperature and the critical temperature. The method Lyndersen-Joback-Reid method is summarized by the following four equations.

$$T_b = 198.2 + \sum n\Delta T_{b_M} \quad (2.1)$$

$$T_c = \frac{T_b}{A_M + B_M\sum n\Delta T_M - (\sum n\Delta T_M)^2} \quad (2.2)$$

$$P_c = \frac{M}{(C_M + \sum n\Delta P_M)^2} \quad (2.3)$$

$$V_c = E_M + \sum n\Delta V_M \quad (2.4)$$

In these equations, n is the number of times that a group appears in the molecules, T_b is the normal boiling temperature, ΔT_{bM} is the contribution to the normal boiling temperature, T_c is the critical temperature, ΔT_M is the contribution to critical temperature, P_c is the critical pressure, ΔP_M is the contribution to the critical pressure, V_c is the critical volume, ΔV_M is the contribution to the critical volume, M is the molecular mass, and A_M, B_M, C_M and E_M are constants. The values of these constant are $A_M = 0.5703$, $B_M = 1.0121$, $C_M = 0.2573$, and $E_M = 6.75$. The values of the contributions to T_b, T_c, P_c , and V_c are summarized in Table 2.6.

Table 2.6 Groups considered for the Modified Lydersen-Joback-Reid method

Groups	ΔT_{bM}(K)	ΔT_M(K)	ΔP_M(bar)	ΔV_M (cm^3/mol)
Without rings				
$-CH_3$	23.58	0.0275	0.3031	66.81
$-CH_2-$	22.88	0.0159	0.2165	57.11
>CH-	21.74	0.0002	0.1140	45.70
>C<	18.18	-0.0206	0.0539	21.78
=CH2	24.96	0.0170	0.2493	60.37
=CH-	18.25	0.0182	0.1866	49.92
=C<	24.14	-0.0003	0.0832	34.90
=C=	26.15	-0.0029	0.0934	33.85
≡CH		0.0078	0.1429	43.97
≡C-		0.0078	0.1429	43.97
-OH (alcohol)	92.88	0.0723	0.1343	30.40
-O-	22.42	0.0051	0.1300	15.61
>C=O	94.97	0.0247	0.2341	69.76
-CHO	72.24	0.0294	0.3128	77.46
-COOH	169.06	0.0853	0.4537	88.60
-COO-	81.10	0.0377	0.4139	84.76
HCOO-		0.0360	0.4752	97.77
=O (others)	-10.50	0.0273	0.2042	44.03
-NH2	73.23	0.0364	0.1692	49.10
>NH	50.17	0.0119	0.0322	78.96
>N-	11.74	-0.0028	0.0304	26.70
-N=	74.60	0.0172	0.1541	45.54
-CN	125.66	0.0506	0.3697	89.32
-NO2	152.54	0.0448	0.4529	123.62
-F	-0.03	0.0228	0.2912	31.47
-CL	38.13	0.0188	0.3738	62.08
-Br	66.86	0.0124	0.5799	76.60
-I	93.84	0.0148	0.9174	100.79
With rings				
-CH2-	27.15	0.0116	0.1982	51.64
>CH-	27.18	0.0081	0.1773	30.56
=CH-	26.73	0.0114	0.1693	42.55
>C<	21.32	-0.0180	0.0139	17.62
=C<	31.01	0.0051	0.0955	31.28
-O-	31.22	0.0138	0.1371	17.41
-OH (phenol)	76.34	0.0291	0.0493	-17.44
>NH	52.82	0.0244	0.0724	27.61
>N-		0.0063	0.0538	25.17
-N=	57.55	-0.0011	0.0559	42.15

Since no experimental critical properties were available to evaluate the accuracy of the estimated values, the liquid density of the ionic liquids are determined as consistency test for the estimated properties using a generalized correlation based on the equation of Spencer and Danner (Spencer and Danner, 1972), which requires only the normal boiling temperature, the molecular weight, and the critical properties.

$$\rho_L = \frac{MP_c}{RT_c}\frac{(0.3445P_cV_c^{1.0135})\Omega}{(RT_c)} \tag{2.5}$$

$$\Omega = -\frac{(1+(1-T_R)^{2/7})}{(1+(1-T_{bR})^{2/7})} \tag{2.6}$$

In these equations, ρ_L is the liquid density (g/cm^3), R is the universal ideal gas constant, T_R is the reduced temperature ($T_R = T/T_C$), and T_{bR} is the reduced temperature at the normal boiling point ($T_{bR} = T_b/T_c$).

Not only the critical properties but also the acentric factor (ω) of the ionic liquids is required in order to calculate the parameters of the equation of state. The acentric factor is calculated by the following expression derived from the definition of this property:

$$\omega = \frac{(T_b-43)(T_c-43)}{(Tc-Tb)(0.7Tc-43)}\log(P_c/P_b) - \frac{(T_c-43)}{(T_c-T_b)}\log(P_c/P_b) + \log(P_c/P_b) - 1 \tag{2.7}$$

In this equation, the calculated critical properties and the calculated normal boiling point temperature are needed. The normal boiling temperature is considered at the normal boiling pressure (P_b = 1.01325 bar).

Valderrama and Robles (2007) determined the critical properties (Tc, Pc, Vc), the normal boiling temperatures (Tb), and the acentric factors (ω) of 50 ionic liquids using an extended group contribution methods based on the

well-known concepts of Lydersen and of Joback-Reid. As for the accuracy and consistency of the estimated value, the liquid density calculation was performed to test the estimation. The results showed that the estimated critical properties, normal boiling temperature, and acentric factors were acceptable for engineering calculations, for generalized correlation, and for equation of state methods with the average deviation and the average absolute deviation of 1.6 and 5.2 %, respectively. Valderrama *et al.* (2008) further determined these properties for 200 ionic liquids and summarized some statistical values, such as the average, absolute, and the maximum deviations observed between predicted and experimental densities. The overall deviations were less than -0.4 % and the overall absolute deviations were less than 5.9 %, whereas only 36 of the 200 ionic liquids presented deviations greater than 10 %.

2.6.2 Equation of State (EoS)

Numerous industrial applications require knowledge of the phase equilibrium mixtures. The phase equilibra can be predicted from a proper thermodynamic model. Such models are necessary to correlate existing experimental data and to predict phase equilibra in regions where experimental data are not available. An equation of state is a thermodynamic equation describing the state of matter under a given set of physical conditions. The equation provides a mathematical relationship between two or more state functions with the matter such as pressure, volume and temperature. In general, cubic equation of state give pressure in terms of volume and temperature of substance are the most commonly used models to predict phase equilibra. Several equations of state have been proposed such as the van der Waals equation, the Redich-Kwong (RK) equation, the Soave-Redlich-Kwong (SRK) equation, the Peng-Robinson (PR) equation. Of all equations, the van der Waals equation is the most important since this model provides a basis for the rest of equation of state. All cubic equation of state contains two constants which are an attractive parameter (a) and a repulsion parameter (b). Hence, they are named two-constant equations of state. The latter parameter involving repulsion also refers to the co-volume parameter which is sometimes called the effective molecular volume. Computation by the cubic equations of state with a

relevant mixing rule can yield a reasonable prediction for vapor-liquid equilibrium of fluids (Walas, 1985; Sandler, 1999; Mushrif, 2004). With respect to multi-component mixture, binary interaction in the mixing rule, which take into account the difference in the interaction of unlike molecules, were optimized from phase-equilibrium data regression, such as VLE data. In general, the interaction parameters have some kinds of temperature dependency. The dependency of temperature is usually a linear function, although in some case polynomials could be used.

One of the main advantages of using the equations of state is that they are straightforward to use and they are present in any process simulator. In most cases, several parameters including temperature, pressure, and composition are required for ionic liquid calculations. However, the equations of state are missing some important parts of the physical nature of ionic liquids. For example, the cations and anions of ionic liquids are considered as a neutral pair, but they still exhibit the presence of polarity and hydrogen bonding ability. Nevertheless, the equations of state do not take these two facts into account. Moreover, the equations of state present a major drawback since they require critical parameters of ionic liquids which can be only obtained indirectly and with large uncertainties. These equations can be used for correlation purposes but the predictive ability is limited by this fact (Vega *et al.*, 2010). This section will provide and discuss sets of equation for the standard Peng-Robinson (PR-EoS), and the Redlich-Kwong-Aspen (SRK-EoS) equations of state, which are available in the Aspen Plus simulator.

2.6.2.1 The Standard Peng-Robinson Equation of State (PR-EoS)

Peng and Robinson (1976) developed the equation of state in which the attractive pressure term of the semi-empirical van der Waals equation has been modified. In Aspen Plus, the standard Peng-Robinson equation of state is the original formulation of the Peng-Robinson equation of state with the standard alpha function. It is also recommended for hydrocarbon processing applications such as gas processing, refinery, and petrochemical processes. The standard Peng-Robinson equation of state (PR-EoS) is proposed as follows:

$$P = \frac{RT}{V_m - b} - \frac{a\alpha}{V^2_m + 2bV_m - b^2} \quad (2.8)$$

The pure component parameters; a and b, for the PR-EoS are calculated by Equation 2.9 and 2.10, respectively.

$$a = \frac{0.457235R^2T_c^2}{p_c} \quad (2.9)$$

$$b = \frac{0.077796RT_c}{p_c} \quad (2.10)$$

The parameter α_i is a function of temperature. It was generally introduced by Soave (1972) in the Redlich-Kwong equation of state. This parameter improves the correlation of the pure component vapor pressure. The relationship between α_i and T_r can be linearized by the Equation 2.11.

$$\alpha = (1+ \kappa(1 - T_r^{0.5}))^2 \quad (2.11)$$

The parameter κ can be correlated against the acentric factor as shown in Equation 2.12.

$$\kappa = 0.37464 + 1.54226\omega - 0.26992\omega^2 \quad (2.12)$$

The mixing parameters; a and b, for the standard PR-EoS are defined by the mixing rules as shown in Equation 2.13, and 2.14, respectively.

$$a = \sum_i\sum_j x_i x_j (a_i a_j)^{0.5}(1- k_{ij}) \quad (2.13)$$

$$b = \sum_i x_i b_i \quad (2.14)$$

In these equation, k_{ij} is a binary interaction parameter, where $k_{ij} = k_{ji}$. For the standard PR -EoS, k_{ij} is temperature dependent term, as shown in Equation 2.15.

$$k_{ij}^{(1)} = k_{ij}^{(2)}T + k_{ij}^{(3)}/T \quad (2.15)$$

$$k_{ij} = k_{ji} \quad (2.16)$$

Also, a linear function of k_{ij} depending on temperature will be taken into account.

2.6.2.2 The Redlich-Kwong-Aspen

In Aspen Plus, the Redlich-Kwong Aspen equation of state is the basis for the RK-ASPEN property method. It can be used for hydrocarbon processing applications. It is also used for more polar components and mixtures of hydrocarbons, and for light gases at mèdium to high pressure. The two-parameter cubic equation of RK-ASPEN is based on a theory of the Soave-Redlich-Kwong (SRK) equation which was derived from the Redlich-Kwong (RK) equation of state (Redlich and Kwong, 1949) and further developed by Soave (1972). The following equation of the SRK-EOS is expressed with a more general temperature dependent term a(T):

$$P = \frac{RT}{Vm - b} - \frac{a\alpha}{Vm(Vm + b)} \quad (2.17)$$

The pure component parameters for SRK-EoS are calculated by Equation 2.18 and 2.19.

$$a = \frac{0.427R^2Tc^2}{P_c} \quad (2.18)$$

$$b = \frac{0.08664RT_c}{P_c} \quad (2.19)$$

The parameter α_i is a temperature function introduced by Soave (1972) in the RK-EoS to enhance the correlation of the component vapor pressure:

$$\alpha = (1 + \kappa(1 - T_r^{0.5}))^2 \tag{2.20}$$

Replacing with parameter κ, parameter α_i will be expressed in the form of the correlation with the acentric factor, as shown in Equation 2.21.

$$\alpha = (1 + (0.48508 + 1.55171\omega - 0.15613\omega^2)(1 - T_r^{0.5}))^2 \tag{2.21}$$

For multi-component equilibra, mixing rules and combining rules which relate to the properties of the pure components and the mixtures are applied. The mixture parameters in liquid phase are calculated from the so-called quadratic mixing rules, as shown in Equations 2.22 and 2.23.

$$a = \sum_i \sum_j x_i x_j (a_i a_j)^{0.5} (1 - k_{a,ij}) \tag{2.22}$$

$$b = \sum_i \sum_j x_i x_j \frac{(b_i + b_j)}{2} (1 - k_{b,ij}) \tag{2.23}$$

$ka_{,ij}$ and $kb_{,ij}$ in equation 2.22 and 2.23 are binary interaction parameters. In the Redlich-Kwong-Aspen equation of state, the interaction parameters are linearly temperature dependent, as shown in Equations 2.24 and 2.25.

$$k_{a,ij} = k^0_{a,ij} + k^1_{a,ij} \frac{T}{1000} \tag{2.24}$$

$$K_{b,ij} = k^0_{b,ij} + k^1_{b,ij} \frac{T}{1000} \tag{2.25}$$

In these equations, parameters ka,ij^0, ka,ij^1, kb,ij^0 and kb,ij^1 are constant.

2.6.3 Activity Coefficient Model

As a result of the limitations mentioned previously for the equations of state, several excess Gibbss free energy models, such as the Wilson's equation, the Non-Random Two-Liquid (NRTL), and the Universal Quasi-Chemical (UNIQUAC), have been used to describe the system involving ionic liquids (Vega *et al.*, 2010). In this work, we did regression on the CO_2 solubility data using the NRTL model.

2.6.3.1 The Non-Random Two-Liquid (NRTL)

The NRTL model is an activity coefficient model that correlates the activity coefficient of a compound with its mole fraction in the liquid phase concerned. In Aspen Plus, the NRTL model will calculate the liquid activity coefficients. It is recommended for highly non-ideal chemical system, and can be used for VLE and LLE applications. The model for the derivation of the NRTL equation of excess Gibbs's free energy is a two-cell theory. The assumption is that the liquid has a structure made up of molecules of type 1 or of type 2 being surrounded proportionally by molecules of both types in a binary mixture. Gibbss free energies of interaction between molecules, g_{ij} are defined, where subscript j refers to the central molecule (Walas, 1985). The concept of NRTL is that the local concentration around a molecule is different from the bulk concentration. This is due to a difference between the interaction energy of the central molecule with the molecules of its own kind g_{ii} and that with molecule of the other kind g_{ij}. The energy difference introduces non-randomness at the local molecular level.

The binary activity coefficients of the NRTL model are given by Equations 2.26 and 2.27.

$$\ln \gamma_1 = x^2_2 \left[\frac{T_{21}(G_{21})^2}{(x_1 + x_2 G_{21})^2} + \frac{(T_{12}G_{12})}{(x_2 + x_1 G_{12})^2} \right] \qquad (2.26)$$

$$\ln \gamma_2 = x^2_1 \left[\frac{T_{12}(G_{12})^2}{(x_2 + x_1 G_{12})^2} + \frac{(T_{21}G_{21})}{(x_1 + x_2 G_{21})^2} \right] \qquad (2.27)$$

Where, G_{12}, G_{21}, T_{12} and T_{21} are calculated by Equations 2.28, 2.29, 2.30 and 2.31, respectively.

$$G_{12} = -\alpha_{12}T_{12} \tag{2.28}$$

$$G_{21} = -\alpha_{21}T_{21} \tag{2.29}$$

$$T_{12} = \frac{\Delta g_{12}}{RT} = \frac{U_{12} - U_{22}}{RT} \tag{2.30}$$

$$T_{21} = \frac{\Delta g_{21}}{RT} = \frac{U_{21} - U_{22}}{RT} \tag{2.31}$$

In these equation, the Gibbs's free energies of the pure substances, g_{12} and g_{21}, are presumed to be equivalent ($g_{12} = g_{21}$). τ_{12}, τ_{21} and α_{12} are three binary parameters adjusted to the experimental solubility data of ionic liquids. In general τ_{12} and τ_{21} are temperature dependent, while α_{12} is usually set as a constant unique value ($\alpha_{12} = \alpha_{21}$). The parameter α_{12} depends on the chemical nature, which is assumed to be characteristic of the non-randomness of the mixture. It is typically in a range of 0.2-0.47, but mostly set as a value of 0.3. It was reported that the correlation with $\alpha_{12} = 0.3$ produced more accurate results according to root-mean-square deviation (rmsd) values (Al-Rashed *et al.*, 2012).

2.6.4 Henry's Law Constant

In 1803, William Henry stated that at a constant temperature, the amount of a given gas that dissolves in a given type and volume of liquid is directly proportional to the partial pressure of that gas in equilibrium with that liquid. An equivalent meaning of this statement is that the solubility of a gas in liquid is directly proportional to the partial pressure of the gas above the liquid. Henry's law constant can be defined in several ways. According to Husson-Borge *et al.* (2003), the Henry's law constant is defined as shown in Equation 2.32.

$$H_{2,1}(p,T) = \lim_{x_2} \frac{f_2(p,T,y)}{x_2} \tag{2.32}$$

In this work, we define an ionic liquid as component 1 and CO_2 as component 2. Therefore, $f_2L(p_2,T,x_2)$ is the fugacity of CO_2 dissolved in the ionic liquid phase, x_2 is the mole fraction of CO_2 in the liquid phase, p_2 is the partial pressure of CO_2 and T is the temperature. At equilibrium, the fugacity of each component in the liquid phase equals to those in the vapor phase, which can be expressed as shown in Equation 2.33.

$$f_2^{liq}(p,T,x_2) = f_2^{vap}(p,T,y_2) = \phi_2(p,T,y_2)y_2p \qquad (2.33)$$

Where $\phi(p_2,T,y_2)$ is the fugacity coefficient of CO_2 as shown in Equation 2.34. For the (ionic liquid + CO_2) system, the ionic liquid is considered to have negligible vapor pressure.

$$\Phi_2(p,T,y_2)y_2p = \phi_2(p,T)p \qquad (2.34)$$

For very low concentrations of CO_2 in the ionic liquid, Henry's law constant can be expressed as in Equation 2.35.

$$H_{2,1}(p,T) = \lim_{x2} \frac{f_2(p,T,y_2)}{x_2} = \lim x_2 \frac{\phi_2(p,T)p}{x_2} \approx \frac{\phi_2(p,T)p}{x_2} \qquad (2.35)$$

According to Anthony (2004), the Henry's law constant, in general, shows the dependency on temperature. However, it is relatively intensive to pressure, especially over a range of low pressure. For an ideal system, knowing the fugacity of CO_2 in the CO_2 phase is able to approximate the gas phase fugacity as the gas phase pressure. The following form of Henry's law can be obtained by Equation 2.36.

$$p_2 = H_{2,1}(T)x_2 \qquad (2.36)$$

Where $H_{2,1}(T)$ has a unit of pressure and is inversely proportional to the mole fraction of CO_2 in the ionic liquid.

2.6.5 Chemical Equilibrium and the Equilibrium Constant

The concept of chemical equilibrium was developed after Berthollet (1803) found that some chemical reactions are reversible. For any reaction mixture to exist at equilibrium, the rates of the forward and backward (reverse) reactions are equal. In the following chemical equation as shown in equation 2.37 to indicate equilibrium, A and B are chemical reactant species, C and D are product species, and a, b, c, and d are the stoichiometric coefficients of the respective reactants and products:

$$aA + bB \leftrightarrow cC + dD \tag{2.37}$$

The equilibrium position of a reaction is said to lie "far to the right" if, at equilibrium, nearly all the reactants are consumed. Conversely the equilibrium position is said to be "far to the left" if hardly any product is formed from the reactants.

The equilibrium constant, Kc, is the ratio of the equilibrium concentration of products over the equilibrium concentrations of reactants each raised to the power of their stoichiometric coefficient as follows:

$$K_c = \frac{[C]^c[D]^d}{[A]^a[B]^b} \tag{2.38}$$

[C], [D], [A], and [B] represent the molar concentration of species C, D, A, and B at equilibrium. For a given reaction, the concentrations at equilibrium would have to be determined experimentally. Value of Kc depends on the temperature, but does not depend on the initial concentrations of reactants and products.

Magnitude of Kc can be described as follows:

1) If the Kc value is large ($Kc >> 1$), the equilibrium lies to the right and the reaction mixture contains mostly products.

2) If the Kc value is small (Kc << 1), the equilibrium lies to the left and the reaction mixture contains mostly reactants.

3) If the Kc value is close to 1 (0.10 < Kc < 1), the mixture contains appreciable amounts of both reactants and products.

2.7 Literature Review

The primary amine especially monoethanolamine (MEA) is the most common solvent used to capture carbon dioxide from post-combustion (PC) system (Baltus *et al.*, 2005). About 75-90 % of the carbon dioxide is captured using MEA-based technology, producing a gas with high purity of carbon dioxide (>99 %) (Rao and Rubin, 2002). However, the CO_2 absorption using MEA present some drawsbacks; high volatility, equipment corrosion and intensive energy usuage during the regeneration step (Ma'mum *et al.*, 2005).

According to the stateDepartment of Energy (DOE), the post combustion CO_2 capture process should be able to achieve 90 % of CO_2 and limit the increase in cost of electricity to less than 35 %. However, the current situation of amine-based scrubbing system does not meet the regulations in terms of energy requirement, stated by DOE (Shiflett *et al.*, 2010)

Among the alternative technologies for CO_2 capture, ionic liquid (IL) has recently attracted widespread attention for CO_2 capture because of their unique properties such as non-volatility, high thermal stability and tunability of their structure and properties. The rivailing of ionic liquid for CO_2 capture with conventioanl amine system can be seen due to their non-volatility. Because of lower vapor pressure of ILs compared to MEA, lower energy requirment during regeneration step can be observed (Wapple *et al.*, 2010)

Shiflett *et al.* (2010) compared the energy requirement and economic investment between MEA and IL-based for post combustion CO_2 capture using 1-butyl-3-methylimidazolium acetate [bmim][Ac] as IL solvent. The results show that [bmim][Ac] can reduce energy usage by about 16 %, the investment about 11 % and the equipment size about 12 %. This is an example that confirms the feasibility of IL for post combustion CO_2 capture when compared with MEA.

Maginn *et al.* (2004) investigated the possibility of using ionic liquid for PC CO_2 capture process by modeling to reach the economic viability. Ionic liquid "100X' which is assumed to be a physical solvent with 100 times the capacity of base-ILs is used for the simulation. Without any process optimization and assuming realistic properties of the liquid, the results indicate that ILs have the potential to be more economically attractive than MEA-based systems.

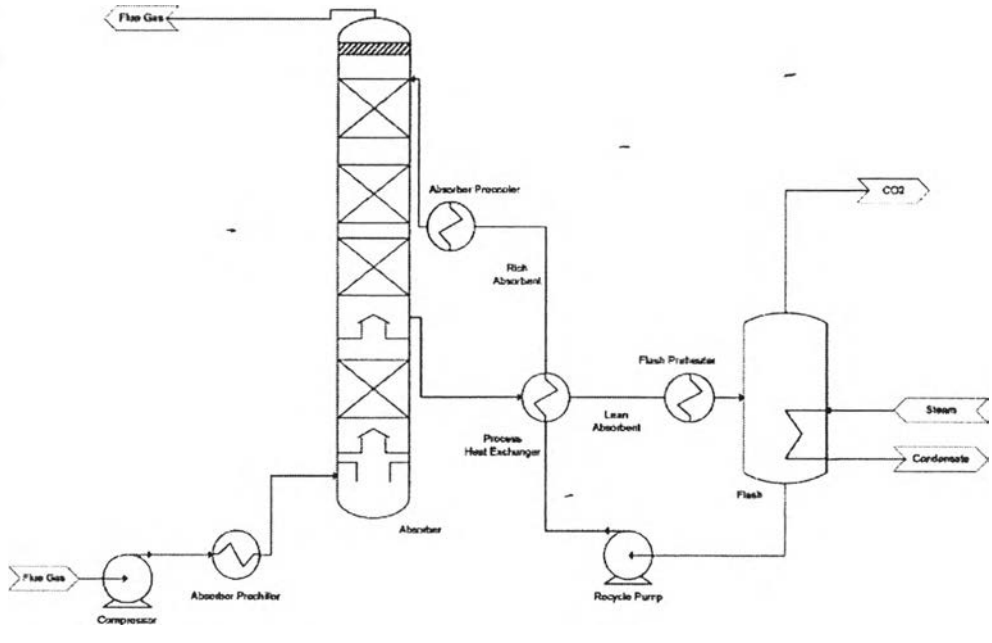

Figure 2.14 IL-based scrubbing process flow diagram (Shiflett *et al.*, 2010).

Many researchers have studied on [bmim][Ac]. Shiflett *et al.* (2008) studied phase behavior of (CO2 + [bmim][Ac]) mixtures. The [bmim][Ac] shows an extremely rare phase behavior ,which CO_2 solubility is highly asymmetric with respect to CO_2 concentration. At low CO_2 concentration (below 20 mol %), hardly any vapor was observed, reflecting a strong attractive interaction (chemical absorption) between CO_2 and [bmim][Ac]. Furthermore, the study of thermodynamic excess function (excess Gibbs free energy, enthalpy and entropy) was done to ensure the presence of chemical absorption between [bmim][Ac] and CO_2. The result shows all large negative excess functions, thus clearly indicating the possibility of intermolecular complex formations or chemical reaction.

Besides the study of Shiflett *et al.* (2008), Maginn (2005) reported the solubility of CO_2 in [bmim][Ac] in terms of Henry's law constant. The acetate anion shows very low Henry's law constant, indicating the complex formation between [bmim][Ac] and CO_2. Moreover, Maginn (2005) also showed the intermolecular complex formations (chemical reaction) mechanism between [bmim][Ac] and CO_2, as shown in Figure 2.15.

Shiflett *et al.* (2009) studied the solubility (vapor-liquid equilibria) of CO_2 for two ILs, 1-ethyl-3-methylimidazolium acetate [emim][Ac] and 1-ethyl-3-methylimidazolium trifluoroacetate [emim][TFA]. The results show that [emim][Ac] has strong chemical CO_2 absorption with low vapor pressure above the mixture with 20 mol % fraction of CO_2. The result of using [emim][Ac] is similar to one of using [bmim][Ac] that had been done before. However, the [emim][TFA] show physical absorption on CO_2.

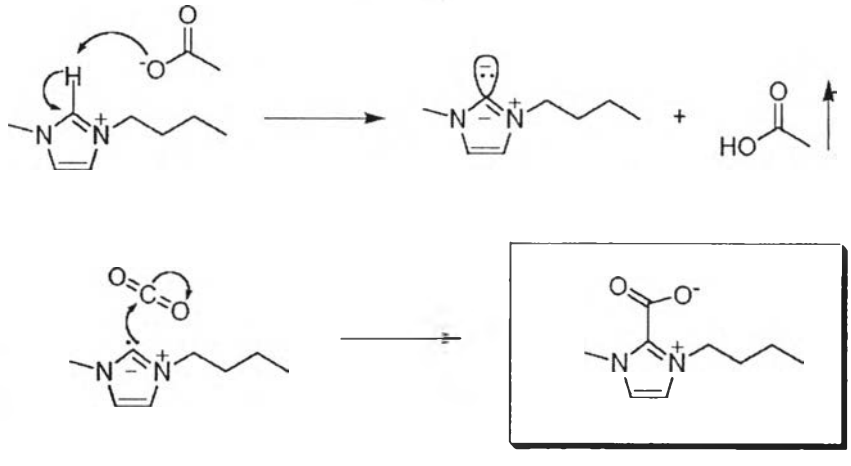

Figure 2.15 Proposed chemical reaction of [emim][Ac] by (Maginn *et al.*, 2005).

The effect of pressure and temperature on CO_2 solubility in IL was studied and the same trends of CO_2 solubility were observed in most studies. It has been established that CO_2 solubility increased with an increase of pressure and decrease of temperature.

Kim *et al.* (2011) studied the solubility of CO_2 in 1-butyl-3-methylimidazolium hexafluorophosphate [bmim][PF6]. The result shows an

increase of CO_2 solubility when pressure is increased and temperature is decreased. This can be confirmed by CO_2 solubility data of Anthony *et al.* (2002) in [bmim][PF6] ,the CO_2 solubility decreased with an increasing in temperature.

Due to the tunability of ILs, the combination between cation and anion can create many types of ionic liquid with different properties. The choice of cation is responsible to their property and stability, while anion is responsible to the impact on chemistry and functionality (such as gas solubility). Imidazolium, phosphonium, ammonium and pyridinium are the example of cation which widely received attention in CO_2 separation, while anions include triflate (TfO), dicyanamide (DCA), tetrafluoroborate (BF_4) and bis(trifluoromethane)sulfonimide (Tf_2N) (Bara *et al.*, 2009).

The tunability on the structure of ILs leads to many studies published on the effect of structural variations of ILs on CO_2 solubility.

Aki *et al.* (2004) studied the solubility of CO_2 in ILs at high pressure up to 150 bar. His study can be divided into four sections; the effect of pressure and temperature on CO_2 solubility in ILs using [bmim][Tf_2N]; the effect of anion on CO_2 solubility in imidazolium-based ILs, using 7 different types of anion including [BF_4^-], [PF_6^-], [TfO^-], [NO_3^-], [Tf_2N^-], [methide] and [DCA]; the effect of alkyl chain length on the cation using three ILs, [hmim][Tf_2N], [hmmim][Tf_2N] and [omim][Tf_2N], and the effect of substitution at C2 position.

For the first study, the consistence was observed with the other literature. The solubility of CO_2 is increased with increasing pressure and decreasing temperature. They also concluded that enthalpy can represent the strength of interaction between IL and gas, and the entropy provides a measure of effect of the dissolved gas on the liquid structure.

The effect of anion shows that the highest solubility of CO_2 are in IL_S with anion containing fluoroalkyl group, [TfO^-], [Tf_2N^-] and [methide]; and lowest solubility in two ILs with nonfluorinated anion, [NO_3] and [DCA]. In fact, CO_2 solubility increase with increasing number of CF_3 groups in the anion.

The results of alkyl chain length show that the CO_2 solubility increases with an increasing in the alkyl chain length at all pressure (0.72 mole fraction for [hmim][Tf_2N] and 0.763 for [omim][Tf_2N] at instance pressure). They concluded

that the density of ILs is decreased with an increasing of alkyl chain length, thus would anticipate greater free volume in the ILs and hence an increasing of CO_2 solubility.

The effect of C2 substitution shows that the substitution of methyl group replacing hydrogen atom at C2 position causes slightly decreasing in CO_2 solubility. CO_2 solubility of [hmmim][Tf_2N] is slightly lower than [hmim][Tf_2N].

Sanchez (2008), studied the anion effect on the CO_2 solubility and concluded that anion had an impact on CO_2 solubility due to the strength of the interaction between CO_2 and anions. He also concluded that, anion modifications that enhance CO_2 solubility (decrease Henry's law constant) included the presence of fluoroine-containing anions and longer alkyl chain length.

Sumon and Henni (2011) also studied the effect of structure on CO_2 solubility. Based on the anion modification, the increase in alkyl chain length of the cation; the alkylation of ammonium and phosphonium cation; changing the cation family from imidazolium to pyridium and pyrrolidinium; and the substitution on C2 position of the cation, are all the solutions that increase CO_2 solubility. Likewise, anions with the presence of fluorine atom show high solubililty of CO_2 ([$MeSO_4$]<[BF_4]<[$OcSO_4$]<[PF_6]<[Tf_2N]). They also studied the effect of molar volume and polarity. The increasing of CO_2 solubility is observed when molar volume is increased and polarity of the ionic liquid is decreased. The selectivity of CO_2 in ionic of the gas mixture (CO_2 + N_2) is decreased when the temperature is increased. The selectivity is also affected by the anion. Fluorine-containing anions are comparatively low on the selectivity, while high in the ILs such as [bmim][BF_4] and [bmim][DCA]. The least negative enthalpy of N_2, indicates lower solubility of N_2 in the ionic liquid.

The selectivity of CO_2 in the ILs has also been studied by other researchers. Husson-Borge *et al.* (2003) reported the solubility of CO_2 and O_2 in 1-butyl-3-methylimidazolium tetrafluoroborate [bmim][BF_4]. It was observed that CO_2 is one order of magnitude more soluble in the IL than O_2. This result agrees with Sumon and Henni (2011) who have shown a high selectivity of CO_2 in [bmim][BF_4].

Galan Sanchez (2008) measured the solubility of CO_2, CH_4, C_2H_4, and C_2H_6 with imidazolium, pyridinium and pyrrolinium; and anion, tetrafloroborate [BF_4],

hexafluorophosphate [PF_6],dicyanamide [DCA], thiocyanate [SCN], methysulfate [$MeSO_4$], bis(trifluoro methylsulfonyl)imide [Tf_2N] and trifluoroacetate [TFA]. The results showed that CO_2 exhibited the highest gas solubility combined with a good selectivity of all studied gases.

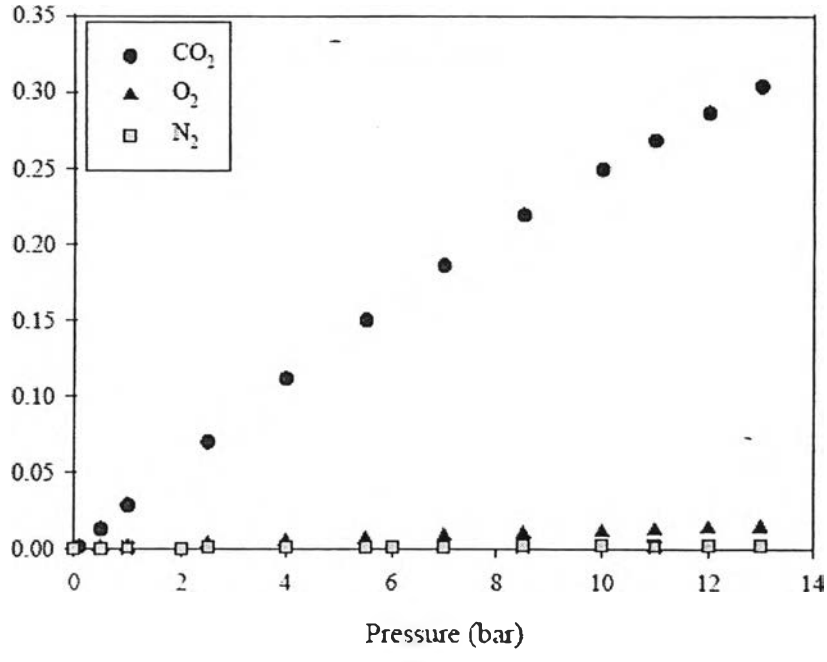

Figure 2.16 Isotherm gas solubility (CO_2, O_2 and N_2) in pyridium-based IL at ambient temperature (Maginn *et al.*, 2004).

Muldoon *et al.* (2007) studied how to improve CO_2 solubility in ILs. They studied an imidazoilum-based IL with the three different levels of fluoronation on anion. The result shows an improvement of CO_2 solubility with increasing number of fluorination: ([bmim][CF_3SO_3]< [bmim][$(CF_3SO_3)_2$]< [bmim][$(CF_3SO_3)_3$]). The fluorination of anion, the replacement of three fluorine atoms with fluoroalkyl group (CF_3) increased CO_2 solubility considerably: ([hmim][PF_6]<[hmim][eFAP]). The solubility of CO_2 in [p5mim][bFAP] is the highest that they have observed for any IL when the dissolution is by physical absorption, in agreement with the study of Sumon and Henni (2011). A similar result was found in Zhang *et al.* (2008). They screened ionic liquid for capture CO_2 by using COSMO-RS method to predict the Henry's law constant of CO_2 in 408 ILs. The screening results show that more CO_2

can be absorbed in ILs with [FEP] anion. It also showed that a value of 0.2 MPa (20 at 0.1 MPa) seems the lowest limit of the Henry's law constant of CO_2 in ILs at 298 K in physical absorption. They also conclued that the [FEP]-based ILs are the most promising candidates for the capture of CO_2 at ambient temperature.

Bara *et al.* (2009) studied CO_2 separation in imidazolium-based room temperature ionic liquids (RTILs). The results show the greatest CO_2 solubility is achieved when the [TF_2N] anion is present, as there is a greater degree of CO_2 interactions with the anion. The other advantages of [Rmim][Tf_2N] are hydrophobic, stable and highyl tunable molten salts (many of [C_2mim][X] salts are hygroscopic and completely miscible in water, thus their performance can change in the presence of water). According to the study of Marsh *et al.* (2004), cation with the [Tf_2N] anion will have low water solubility, while replacing with [BF_4] anion can dramatically increase the water solubility in ILs.

The miscibility of ILs in water is strongly dependent on their anion. Cl^-, Br^-, I^-, NO_3^-, CH_3COO^- and CF_3COO^- are anions that make ILs miscible with water. ILs composed of anion such as PF_6^- and Tf_2N^- are immiscible with water. Miscibility of water of ILs based on anion such as BF_4^- and $CF_3SO_3^-$ is depedent on the structure of the cation, even though they are generally miscible with water. The miscibility is also decreased with the increasing of cation chain length.

Bara *et al.* (2009) also reported the correlation among solubility parameter, CO_2 solubility, CO_2 selectivity and molar volume of ILs. Higher values of solubility parameter and CO_2 selectivity were observed when CO_2 solubility and molar volume of ILs are decreased. The solubility of CO_2 in ILs was found to be at maximum when the ILs solubility parameter was 21.8, which is the solubility parameter of CO_2.

Maginn (2004) studied the solubility of CO_2 and the other gases (N_2, O_2, NO, NO_2, N_2O and SO_2) on nine ILs including 1-n-butyl-3-methylimidazolium acetate, 1-n-hexyl-3-methylimidazolium bis[(trifluoromethyl)sulfony]imide, 1-n-hexyl-3-methylimidazolium tris(pentafluoroethyl)trifluorophosphate, 1-butyl-3-methylimidazolium 2-(2-methoxyethoxy)sulfate, Tetrabutylammonium bis(2-ethylhexyl) sulfosuccinate, 1-methyl-3-(nonafluorohexyl)-imidazolium bis[(trifluoromethyl)sulfony]imide, 1-methyl-3-tetread3ecyfluorooctylimidazolium bis[(trifluoromethyl)sulfony]imide, and 1-n-butyl-3-methylimidazolium

perfluoroctonate using a gravimetric microbalance at the isotherm between 10 and 70 °C. The results show that bis[(trifluoromethyl)sulfony]imide (Tf_2N^-) anion has higher CO_2 solubility than small anion such as tetrafluoroborate (BF_4^-).

Cadena *et al.* (2004) studied CO_2 solubility in six imidazolium-based ILs, 1-butyl-3-methylimidazolium hexafluorophosphate ([bmim][PF6]), 1-butyl-2,3-dimethylimidazolium hexafluorophosphate ([bmmim][PF6]), 1-butyl-3-methylimidazolium tetrafluoroborate ([bmim][BF4]), 1-butyl-2,3-dimethylimidazolium tetrafluoroborate ([bmmim][BF4]), 1-ethyl-3-methylimidazolium bis[(trifluoromethyl)sulfony]imide ([emim][Tf2N]), and 1-ethyl-2,3-dimethylimidazolium bis[(trifluoromethyl)sulfony]imide ([emmim][Tf_2N]) at three isotherms at 10, 20 and 50 °C and pressure up to 13 bar. The results show that (Tf_2N^-) anion has the highest affinity with CO_2. They also conclued that the anion has the greatest impact on the CO_2 solubility, while cation played the secondary role.

Kim *et al.* (2005) studied the CO_2 solubility of six room temperature ionic liquid (RTILs), [bmim][PF_6], [C_6mim][PF_6], [emim][BF_4], [C_6mim][BF_4], [emim][Tf_2N] and [C_6mim][Tf_2N] at 298.15 K and up to 1 MPa. The results show that, 1-hexyl-3-methylimidazolium bis(trifluoromethysulfonyl)imide [hmim][Tf2N] has the highest CO_2 solubility.

Qchedzan-Siodlak *et al.* (2013) studied the viscosity of imidazolium and pyridinium chloroaluminate ILs. The results show that, the viscosity of ILs are decreased with an increasing of temperature. They concluded that molar mass, van der Waals interaction, chain tangling and H-bonding interaction are main factors influencing the viscosity of ILs. Increasing of alkyl chain length makes the ILs more viscous due to the increasing of van der Waals interaction, but not in the linear trend. Based on the imidazolium and pyridinium ILs, increasing of alkyl chain length from C4 to C6 causes the greater change on the viscosity than changing from C6 to C8, but the diverse order can be seen in methylpyridinium-based ILs. Isomer "meta" is found to have higher viscosity than "para".

Sanchez *et al.* (2007) compared the viscosity between conventional solvent for CO_2 capture (MEA) and RTIL. The viscosity of 1-butyl-3-methylimidazolium tetrafluoroborate ([bmim][BF_4]) was 40 times higher compared to aqueous solution of 30 % MEA. Both viscosity of MEA and [bmim][BF_4] decrease with an increasing

of temperature from 30 to 70 °C by the factor of 4.5 for [bmim][BF_4] and 2.7 for MEA. [bmim][BF_4] shows higher decreasing in viscosity compared to MEA at the same temperature range.

Baltus *et al.* (2005) concluded that, the viscosity of imidazolium-based ILs is governed by van der Waals and H-bonding between anion and imidazolium cation ring. For anion [Tf_2N], H-bonding is suppressed, thus van der Waals interaction is the only factor that dictates to the viscosity. Increasing of the alkyl chain length increases van der Waals interaction and causes higher viscosity of ILs. The increasing of viscosity by increasing of alkyl chain length can be explained by the increase in the bulkiness of imidazolium ring with bulkyl functional groups. An increase in bulkiness of the cation reduces the mobility of the cation, therefore increasing the ILs viscosity.

MEA capture process is known as the most feasible process for CO_2 capture technology. Eventhough many efforts have been made to find new technology to replace MEA-based system, these emerging alternative technologies have not become commercial, some of them are even in the research step. So, the optimization of current technology, MEA still required.

Kothandaraman (2005) studied the chemical absorption process by using monoethanolamie, potassium carbonate and chilled ammonia. He also focused on the optimization of MEA-based system, studied the effects that influence the reboiler duty; lean loading (mol CO_2/mol MEA), CO_2 capture percentage, absorber height, solvent temperature, desorber pressure and effect of cross heat exchanger.

Increasing lean loading causes the decreasing in reboiler duty, because less amount of steam has to be applied in the stripper. When the CO_2 percentage is increased, the solvent flow rate needs to increase to maintain the CO_2 recovery. The increase of flow rate causes an increase of sensible heat that leads to higher re-boiler duty. Absorber height is increased causing the decrease of reboiler duty, due to the higher rich loading. Low solvent temperature is appropriate for the absorption process, because it enhances the driving force of the absorption process, but the reaction rate and diffusity are low at low solvent temperature. High desorber pressure is going with high temperature.

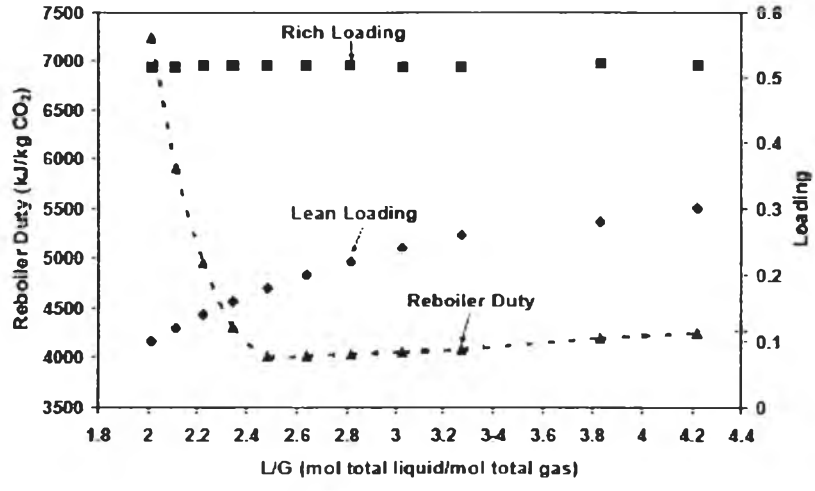

Figure 2.17 Variation of reboiler duty and rich loading with L/G for 85% CO_2 capture from coal flue gas; equilibrium simulation. (Kothandaraman, 2005).

Due to the exothermic reaction of desorption step, the driving force of the absorption will increase with increasing temperature, but the temperature is limited to 122 °C due to the degradation of MEA. The approach temperature of cross-heat exchanger also affects the reboiler duty. Lower approach temperature causes the decrease of re-boiler duty, but larger surface area of heat exchanger. All of these results were confirmed by other studies (Freguia, 2003; Piewkhaow, 2011).

Lu *et al.* (2012) improved MEA-based process by using a mixed absorbent composed of MEA and [bmim][BF4]. The optimum mole ration of MEA to [bmim][BF4] was found to be 7:3 The absorption capacity of the mixed absorbent was significantly higher than pure MEA aqueous, approaching 0.638 mol of CO_2 per mol of MEA. All the results, they concluded that the mixed absorbent employed in their CO_2 capture process can help to improve the stability and reliability of the system, which is beneficial to industrial applications.